CHEMISTRY

A EUROPEAN JOURNAL

6/18 2000

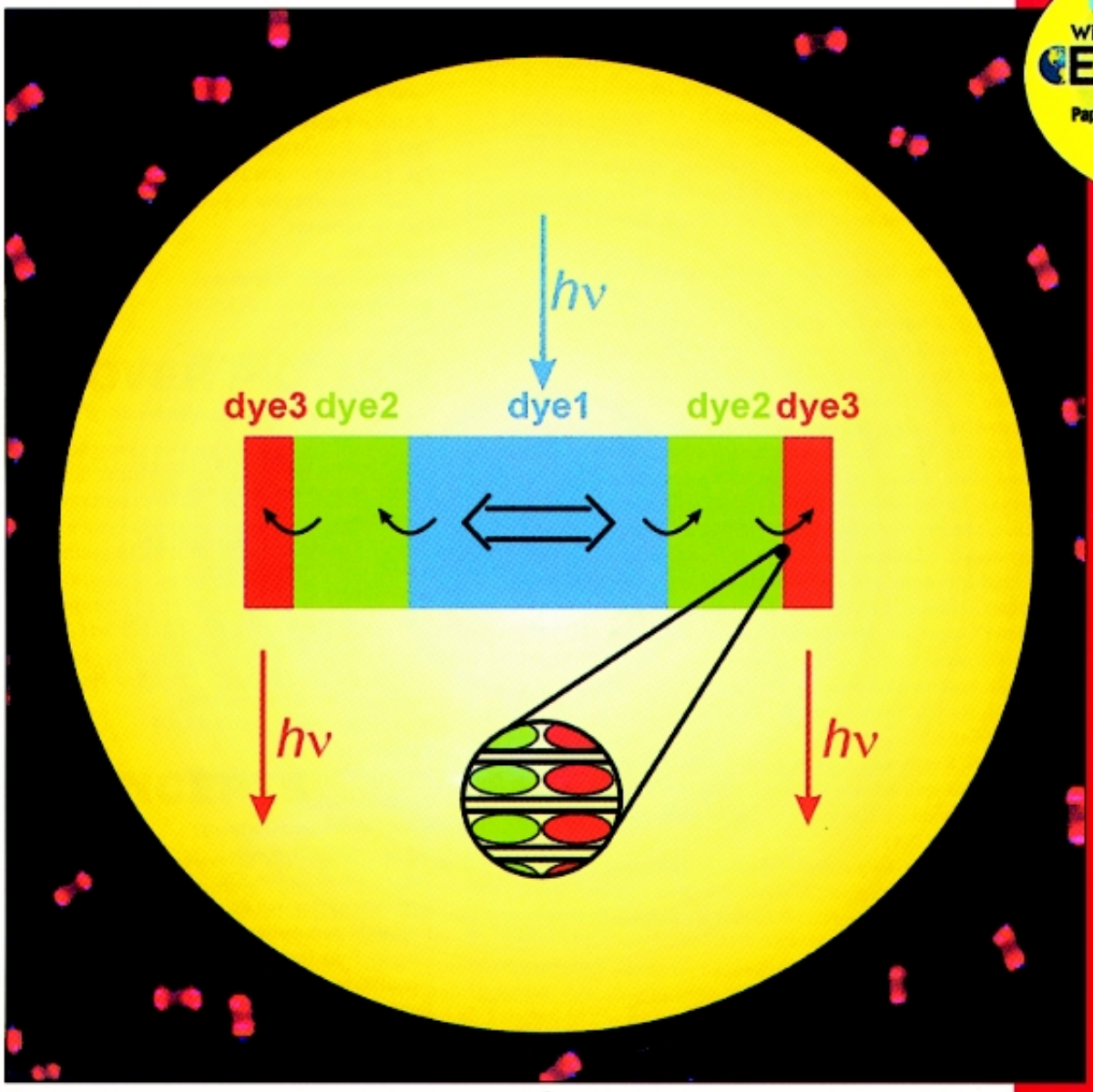

Concepts

A Library of Carbohydrate Mimics and Polyketide Segments for the Synthesis of Marine Natural Products

H. M. R. Hoffmann and A. M. Misske

Multi-Component Transformations Lead the Way

H. Bienaymé et al.

WILEY-VCH

CEUJED 6 (18) 3303–3474 (2000) · ISSN 0947-6539 · Vol. 6 · No. 18 · September 15, 2000

Cover Picture

G. Calzaferri et al.

The cover picture shows a schematic view of a bipolar antenna for light harvesting and transport surrounded by fluorescence microscopy pictures of individual antenna crystals. Zeolite L microcrystals of cylinder morphology are used as host for organising several thousand dyes as monomers into well defined zones. The enlarged section shows the organisation of individual dye molecules at the domain boundary between dye2 and dye3. The microscopy pictures demonstrate the antenna behaviour: They show the red fluorescence of dye3, located at both ends of the crystals, after selective excitation of the blue dye1 in the middle. The synthesis and characterization of these dye loaded zeolite L sandwiches are described by G. Calzaferri et al. on p. 3456ff.

Dye-Loaded Zeolite L Sandwiches as Artificial Antenna Systems for Light Transport

Marc Pauchard, André Devaux, and Gion Calzaferri*[a]

Abstract: The synthesis and characterization of dye loaded zeolite L sandwiches acting as artificial antenna systems for light harvesting and transport is reported. A set of experimental tools for the preparation of neutral dye-zeolite L materials ranging from low to maximum packing densities has been developed. The role of co-adsorbed water and the distribution of molecules between the inner and the outer surface were found to be the determining parameters. *p*-Terphenyl (*p*TP) turned out to be very suitable for studying these and other relevant parameters of neutral dye-zeolite L materials. We observed that *p*TP located in the channels of zeolite L can reversibly be displaced by water. This can be used when synthesizing such materials. We also observed that all-*trans*-1,6-diphenyl-1,3,5-hexatriene (DPH) which is very photolabile in solution is stable after insertion into zeolite L. By combining our extensive knowledge of these systems with ion-exchange procedures developed in an earlier study, we have realized the first bi-directional three-dye antenna. In this material the near UV absorbing compounds DPH or 1,2-bis-(5-methyl-benzoxazol-2-yl)-ethene (MBOXE) are located in the middle part of zeolite L nanocrystals followed on both sides by pyronine (Py) and then by oxonine (Ox) as acceptors. Fluorescence of the oxonine located at both ends of the cylindrical zeolite L crystals was observed upon excitation of the near UV absorber in the middle section at 353 nm, where neither oxonine nor pyronine absorb a significant amount of the excitation light.

Keywords: artificial antenna · energy transfer · host–guest chemistry · supramolecular chemistry · zeolites

Introduction

The structural, morphological, physical, and chemical variety of zeolites has led to applications in different fields such as catalysis,[1] ion exchange, membranes,[2, 3] and chemical sensors where dynamic processes involving ions or adsorbate molecules play an important role. Situations where the zeolites mainly serve as host for supramolecular organization of molecules, ions, complexes, and clusters to prepare materials with new properties such as nonlinear optical,[4] quantum-size,[5, 6] micro laser,[7] and artificial antenna characteristics[8–10] are new fields of growing interest.[11–13] Some of these new materials can be considered as a static and stable arrangement of guests in the zeolite host under a broad range of conditions.[14] In other cases, the adsorption, desorption or ion exchange of molecules or ions are reversible processes which lead to a wide range of phenomena.[15–17]

Our current interest in zeolites is focused on their use as host materials for different kinds of supramolecular organization.[6, 8] This article concentrates on the synthesis of dye-loaded zeolite L sandwiches acting as artificial antenna systems. It has been demonstrated both theoretically and experimentally that by organizing cationic dyes in the one-dimensional channels of zeolite L nanocrystals an artificial antenna system for light harvesting and fast anisotropic energy transport can be realized.[9, 10, 18, 19] In this material two different kinds of dyes with appropriate photophysical properties are organized as monomers in spatially separated domains. The structure of the system allows selective excitation of the central part and fast transport of the energy along the channel axis to the top and bottom faces of the crystals. Pyronine and oxonine have been used as chromophores in this material. Blue-green light is selectively absorbed by the pyronine molecules located in the middle part of the crystals with cylindrical morphology. The energy then migrates to the crystal ends where it is captured by the oxonine and then emitted as red luminescence.

In the presented work neutral molecules absorbing UV light were incorporated in order to evaluate the light harvesting properties of this material. The resulting three-dye zeolite L sandwich materials open the door to new systems with fascinating properties. We show that a bi-directional antenna for light collection and transport can been prepared so that the whole visible light spectrum can be used. The light

[a] Prof. Dr. G. Calzaferri, M. Pauchard, A. Devaux
Department of Chemistry and Biochemistry, University of Bern
Freiestrasse 3, 3012 Bern (Switzerland)
Fax: (+41) 31-6313994
E-mail: gion.calzaferri@iac.unibe.ch

  0947-6539/00/0618-3456 $ 17.50+.50/0

energy is carried spectrally from blue to green to red and spatially from the central part of the crystal to its top and bottom faces. Good candidates as UV absorbers, which also have the right structural characteristics, can be found among the strongly luminescent scintillation dyes and optical brighteners. Existing methods for the synthesis of neutral-dye loaded zeolite materials were not adequate for our purpose. We have therefore elaborated adapted procedures to obtain reproducible, homogeneous, and well defined neutral-dye zeolite L materials with high packing densities.

While the concept of the synthesis procedure is simple, a number of details must be considered when dealing with host–guest zeolite materials. It is important to distinguish between molecules located inside of the channels and those adsorbed at the outer surface of the nanocrystals. The conditions under which such a material can be considered as a static arrangement of guest molecules in a host deserve some attention. As a result of the complexity of these composite materials care must be taken when generalizing results or when using concepts developed in other fields to predict the characteristics of new systems.[20, 21] Fortunately chemical methods in combination with a number of different techniques such as vibrational spectroscopy,[22–24] UV/Vis absorption and luminescence spectroscopy,[14, 17, 25, 26] optical microscopy, nuclear magnetic resonance (NMR),[27] powder neutron diffraction (PND),[28] powder X-ray diffraction (PXD),[24] thermogravimetry (TGA)[29] and others can be used to obtain the necessary information regarding the location of adsorbed molecules and the stability of the materials. A suitable set of experiments was elaborated for the characterization of the materials reported in this article. We will show that co-adsorbed water can play a determining role in the behavior of neutral-dye loaded zeolite L and that it is rather crucial to control this parameter. Some work on the influence of co-adsorbed water on the organic guest distribution in the zeolite host has been reported in the literature,[16, 30–34] while in other cases uncertainties remain because no information concerning this aspect was given.[35]

We report herein the results for the dye molecules shown in Scheme 1. They are of appropriate size for being inserted into the channels of zeolite L. We will show that their behavior with respect to co-adsorbed water is quite specific. The properties of DPH and of MBOXE enabled us to synthesize the first three-dye loaded zeolite L material with bi-directional antenna characteristics.

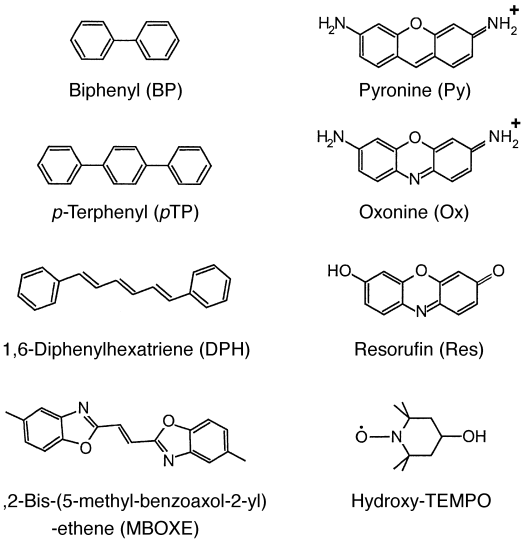

Scheme 1. Molecules discussed in this article.

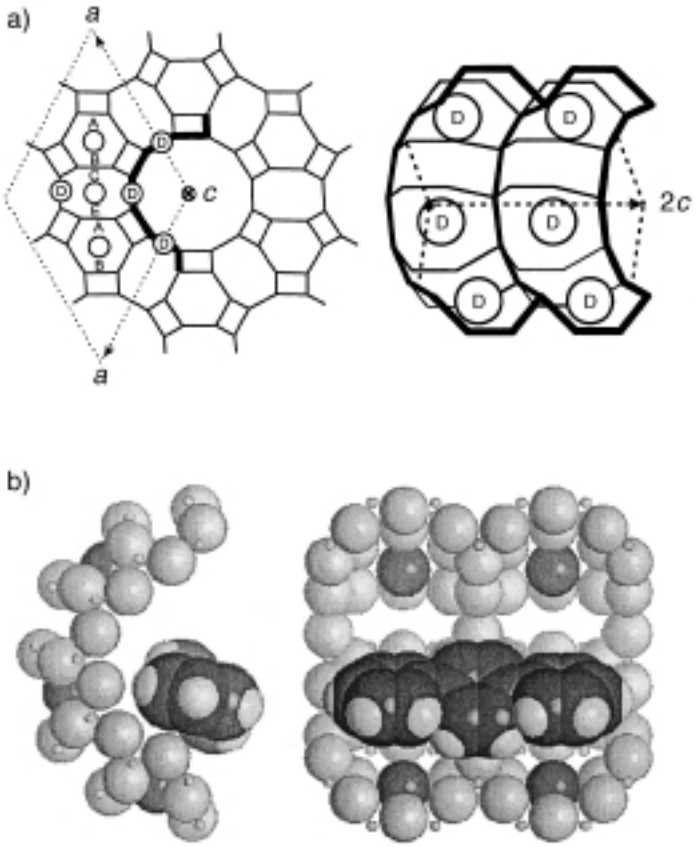

Scheme 2. a) Zeolite L framework with crystallographic axis (*a*,*c*) and different cation positions A to E. b) van der Waals model of a *p*TP molecule in the main channel of zeolite L.

General Discussion

Host: Zeolite L is an aluminosilicate with hexagonal symmetry and a one-dimensional channel system along the *c* axis as illustrated in Scheme 2a).[36, 37] The opening of the main channel consists of a so called 12-membered ring with a free diameter of 7.1–7.8 Å. The 12 bridging oxygen atoms are not counted in this generally accepted nomenclature. In order to compensate for the negative charge due to the aluminium in the framework, up to 10 cations per unit cell (depending on the Si/Al ratio) are distributed over the different cation positions A to E. The largest free channel diameter of $\approx$12.6 Å is influenced by the charge compensating cations at the D positions.[28]

In its hydrated form the zeolites void space is filled with water. The water molecules in the larger zeolite cavities have been reported to practically show the characteristics of the isolated liquid, thus indicating that the molecules in the center of the large cavities do not occupy defined lattice sites. In the smaller cavities, the water molecules appear to cluster around

  0947-6539/00/0618-3457 $ 17.50+.50/0

the cations.[20] Evacuation of air-dry K^+-zeolite L at room temperature leads to desorption of most of the original water. This water is not strongly bound to the sorbent and is apparently localized in the main channels of the zeolite L. Water molecules localized in the secondary system of channels desorb at higher temperatures (>400 °C).[38] It is known that zeolite L is stable under an oxygen atmosphere at temperatures up to 800 °C for several hours.[39] The framework structure varies little with temperature or dehydration and the non framework cation positions do not change significantly upon hydration/dehydration, reduced temperature or adsorption of aromatic molecules.[28]

Adsorption and ion-exchange processes in zeolites are controlled by the size of the channel openings. The size of the diffusing species and the size of the aperture, as derived from a hard-sphere model, are useful to decide if a molecule has a chance to enter a cavitiy or not. In limiting cases this rough picture must be extended by the concept of the kinetic diameter of the channel opening and the diffusing species. Both of them are strongly temperature dependent. It is known that thermally excited ring vibrations of the zeolite, which cause large oxygen amplitudes, play an important role. Thermally excited modes of the diffusing species can be equally important. Similar arguments hold with respect to the question if and under what conditions two species can glide past each other for example in the channels of zeolite L. The inhibition of such counter diffusion for sufficiently large molecules is a critical condition for the synthesis of sandwich structures as described in this article.

In comparison to neutral zeolite types (e.g. $AlPO_4$-5) zeolite L has the advantage of allowing insertion of neutral and of cationic dyes which leads to a higher choice in the palette of molecules and more flexibility for the synthesis of composed structures. Cationic dyes can be inserted in the zeolite channels in the presence of water. For each inserted monovalent dye molecule one alkali cation of the main channel must leave the framework. Neutral molecules can be inserted best when the main channels are water free, because water is in competition with them at the adsorption sites. The way this influences the stability of neutral-dye loaded zeolite L in the presence of water will be discussed in detail.

Guests: Because of its high thermal and photochemical stability the synthesis and characterization methods for neutral dyes were elaborated with *p*TP. The sublimation of *p*TP at 3×10^{-2} mbar starts at 125 °C.[40] Heating for 10 d under air or helium at 390 °C was reported to yield only 3% decomposition products. A typical reaction known from this class of substances, the formation of polycondensation products, is only observable at higher temperatures (>480 °C within 2 d).[41] In Scheme 2b) a van der Waals model of *p*TP in the zeolite L main channel is shown (the torsion angles of *p*TP are chosen (30°, – 30°) corresponding to a mean value reported for biphenyl in solution[42]).

The experience gained with *p*TP was then applied and extended to the neutral molecules reported in Scheme 1. DPH and MBOXE were used together with Py and Ox to synthesize two different three-dye zeolite L sandwich materials. In Figure 1 we show the electronic absorption a) and the normalized emission spectra b) of DPH in 1-butanol and of Py and Ox in water. The arrow indicates the wavelength of the light which can be used to specifically excite DPH in the presence of Py and Ox.

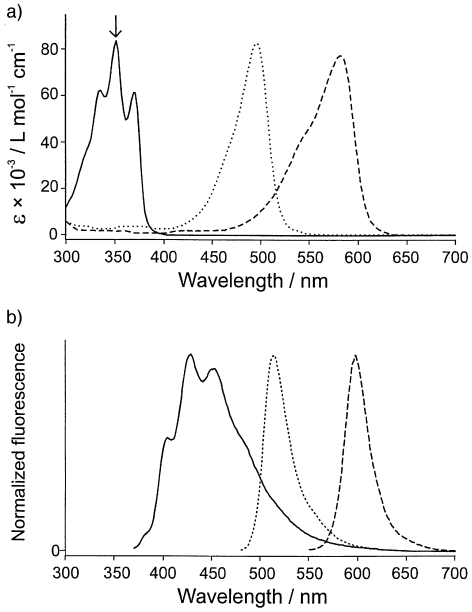

Figure 1. a) Electronic absorption spectra of DPH (solid line) in 1-butanol and of Py (dotted line) and Ox (dashed line) in water (10^{-5} M). The wavelength of 353 nm used for the specific excitation of DPH in the antenna system is indicated by an arrow. b) The corresponding emission spectra of the three solutions (10^{-6} M) were recorded after excitation at the absorption maxima of the individual species ($\lambda_{ex,DPH} = 353$ nm, $\lambda_{ex,Py} = 495$ nm, $\lambda_{ex,Ox} = 582$ nm) and normalized to equal height at the band maxima.

Sandwich structures: The spatial restrictions of the zeolite L host and the characteristics of the used dye molecules allowed the synthesis of sandwich structures. A typical nanocrystal of 800 nm length and a diameter of 1100 nm contains about 300000 parallel one-dimensional channels. The general concept of the synthesis of these materials is illustrated in Scheme 3. First, neutral dye1 molecules are inserted, for example from the gas phase, filling the channels to the desired degree. Provided that the inserted molecules are not rapidly displaced by water, this material can then be subjected to ion exchange from aqueous suspension with dissolved cationic dye2. This process can be well controlled, so that a specifically desired space is left for the third cationic dye3, which is inserted in the same way.

Reactions: When preparing or handling dye loaded zeolite L materials different reactions can play a role: hydration/dehydration of the material, adsorption/desorption of dyes at the inner and outer surface of the nanocrystals, displacement of dyes by water, and reinsertion upon dehydration, cation exchange in case of cationic dyes. It is useful to express the reversible reactions where dyes are involved as follows:

Insertion from the gas phase or melt: Dye molecules in the gas phase or the melt $D(g,m)$ are in equilibrium with dye molecules in the channels of the dehydrated zeolite ZD_r.

0947-6539/00/0618-3458 $ 17.50+.50/0 *Chem. Eur. J.* **2000**, *6*, No. 18

The parameter r counts the number of sites occupied by dye molecules. Its values range from 0 to n_{box}, where n_{box} is equal to the number of sites in one channel. A site represents the part of the main channel which is occupied by an adsorbed dye molecule. The dye molecules are positioned at sites along the linear channels. The sites do not overlap. The length of a site is equal to an integral number u times the crystallographic c axis, so that one dye molecule fits into one site.[43] Each site is occupied with the same probability by a dye molecule. In case of for example a 600 nm long zeolite crystal and a 1.5 nm long dye which occupies two unit cells, n_{box} is equal to 400.

$$ZD_{r-1} + D(g,m) \rightleftharpoons ZD_r \quad (1)$$

Displacement equilibrium: Neutral dye molecules D in the zeolite ZD_rX_{p-x} can be displaced by x molecules X. In this study X is a water molecule. The states of X(out) and D(out) are gas, liquid, solid, or molecules adsorbed at the outer surface of zeolite nanocrystals.

$$ZD_rX_{p-x} + xX(out) \rightleftharpoons ZD_{r-1}X_p + D(out) \quad (2)$$

Ion exchange equilibrium: In the experiments reported in this article monovalent cationic dyes have been used. D_S^+ and M_S^+ denote the dye cation and the alkali metal cation in solution. The parameter n_{box} is equal to the number of sites in one channel and r counts the number of sites occupied by a dye. Y denotes the cation concentration inside the zeolite channels. For monovalent cations and dyes, such as Py and Ox which occupy two unit cells in zeolite L, we must use $Y_{n_{box-r}} = [(M^+_{18n_{box-r}}(M^+_{17})_r]$ to describe the state of a given channel. A site contains 18 cations M^+ and only one of them can be exchanged by a singly charged dye cation D^+. By the exchange of $r \cdot D^+$ molecules the number of sites containing 18 cations, $(M^+_{18})_{n_{box}}$, is reduced by r so that r sites with only 17 alkali cations are formed.[9]

$$ZY_{n_{box-(r-1)}}D_{r-1} + D_S^+ \rightleftharpoons ZY_{n_{box-r}}D_r + M_S^+ \quad (3)$$

Adsorption at the outer surface and insertion of adsorbed cationic dye molecules: Adsorption at the outer surface followed by insertion was discussed by us in some detail for an aqueous suspension of the cationic dye thionine and zeolite L. Thionine and structurally related molecules, such as Py and Ox, have a strong tendency to form so called H-type aggregates on the surface of zeolite crystals.[25, 44] They can be recognized by their different electronic absorption spectra. When a total number t of dye molecules are adsorbed, $\frac{t}{m}$ aggregates $(D^+)_m$ (with $m = 2, 3, \ldots$, i.e., dimers, trimers etc.) can form on the outer surface. The inclusion reaction for these aggregates can then be expressed by Equation (4), where *ads* indicates dyes adsorbed at the outer surface and *cage* indicates dyes inserted in the zeolite L channels.

$$ZM^+_{n-t}\left[\frac{t}{m}(D^+)_m\right]_{ads} \rightleftharpoons ZM^+_{n-t}\left[\left(\frac{t}{m}-1\right)(D^+)_m\right]_{ads}[mD^+]_{cage}$$

$$ZM^+_{n-t}\left[\left(\frac{t}{m}-1\right)(D^+)_m\right]_{ads}[mD_+]_{cage} \rightleftharpoons ZM^+_{n-t}\left[\left(\frac{t}{m}-2\right)(D^+)_m\right]_{ads}[2mD^+]_{cage} \quad (4)$$

Definitions and terminology: The following definitions and expressions have been used: Molecules per unit cell (u.c.) describes the average number of molecules contained in one primitive unit cell when a statistical distribution over the crystal is assumed. As the dye-molecules can only enter the main channels of zeolite L, the unit cell may be reduced to the cavity of the main channel. In Scheme 2b) a loading of 0.5 *p*TP per u.c. is illustrated. The occupation probability p is equal to the ratio between the occupied and the total number of sites. In *hydrated* zeolite L the channels are completely filled with water. The exact amount of water in the framework depends on the Si/Al ratio (which is 3.2 in our case) and on the humidity of the environment in equilibrium with the material. It varies in our case from 16.2 H_2O per u.c. (22% rel. hum.) up to 21.7 H_2O per u.c. (98% rel. hum.). *Dehydrated* zeolite L means zeolite L after the indicated dehydration process. A complete removal of the water was only achieved when heating the zeolite up to 1000 °C in a nitrogen stream, as realized in TGA measurement. Otherwise the zeolite still contains some water adsorbed at the cations in the small cavities. A *dry* dye-zeolite L is a dye-loaded zeolite L after synthesis and without contact to humidity (handling in the glove box). Here some water adsorbed at the cations in the small cavities is also present. *Wet* dye-zeolite L means dry dye-loaded zeolite L exposed to 22% relative humidity until equilibration is achieved. *dye2,dye1*-zeolite L describes a zeolite L sandwich material with dye1 in the middle part and the indicated dye2 at both ends of the crystal. If further modifications are made, the symbol of the next dye is set as prefix to the name (e.g. dye3,dye2,dye1-zeolite L, see Scheme 3).

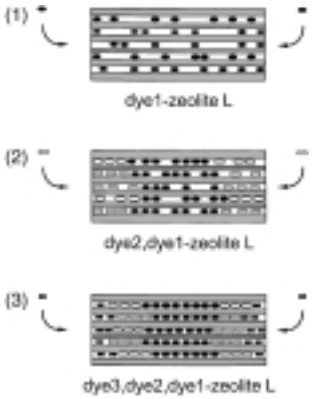

Scheme 3. Insertion of three different dyes into the zeolite framework to form a sandwich material.

Results

*p*TP was found to be an excellent choice for developing the synthesis methods and for studying the relevant parameters. We therefore proceed as follows. First the results obtained with the *p*TP-zeolite L systems are described in detail. In the section on other neutral-dye zeolite L materials (see below) the most important results for the other neutral dyes reported in Scheme 1 are summarized. We then describe properties of the three-dye zeolite L sandwiches which have been used for energy transfer and energy migration experiments.

Insertion of *p*TP into zeolite L—The effectiveness of dehydration

In the double and simple ampoule synthesis methods, described in the Experimental Section, the zeolite has to be dehydrated prior to the adsorption of the neutral molecule. The effectiveness of our procedure was checked by two independent experiments. The argon adsorption isotherms of dehydrated zeolite L gives information about the accessibility of the main channels to the argon molecules and the gravimetry (see Experimental Section) shows how many H_2O per u.c. are contained in such a dehydrated sample. The specific monolayer surface area obtained from the argon adsorption isotherm of the dehydrated zeolite L was equal to the value obtained for the reference sample dehydrated at the Sorptomatic instrument under dynamic vacuum conditions ($< 10^{-4}$ Torr at 300 °C). This shows that the dehydration method used in the sample preparation leads to water free main channels. Gravimetric measurements with dehydrated zeolite L and dry *p*TP-zeolite L showed that about 1 H_2O molecule per u.c. remained in the zeolite after dehydration. It can be concluded that the water remaining in the zeolite L framework after dehydration is present as hydroxyl groups or is located in the smaller side channels where it neither affects the adsorption of argon nor that of *p*TP.

Sample composition determined by TGA: After the insertion of *p*TP into the zeolite channels by one of the methods described in the Experimental Section, the sample was rehydrated and its composition was determined by means of TGA. Figure 2a) shows a desorption curve (TGA) of hydrated zeolite L and its first derivative (DTG) as a function of temperature. In a fast desorption step between 25 and 220 °C up to 95 % of the water leaves the zeolite L framework. The remaining 5 % desorb with a much slower rate between 220 and 1000 °C. The water molecules located in the main channels and those in the smaller cavities can be distinguished by their different desorption behavior. The total amount of desorbed water for hydrated zeolite L is 10.5 ± 0.1 % by weight which corresponds to 16.2 ± 0.2 H_2O per u.c. For the correct determination of the amount of neutral dyes desorbing during a TGA measurement, the desorption of the strongest bound water molecules has to be taken into account. From the TGA of the hydrated zeolite L this amount was calculated to be 0.7 H_2O per u.c. in the interval from 220 °C to 1000 °C.

Figure 2b) shows a typical desorption curve of a wet *p*TP-zeolite L sample. The desorption of water is followed by two distinguishable desorption processes at higher temperature. The desorption starting at 400 °C can be assigned to the loss of *p*TP or reaction products resulting from it. The amount of water desorbing between 25 °C and 220 °C is the same as in the case of hydrated zeolite L. The calculated ratio of *p*TP to zeolite is 0.53 ± 0.02 *p*TP per u.c. The sample composition determined by the TGA is homogeneous and shows no changes over several weeks, when stored at 22 % relative humidity. Figure 2c) shows a reference TGA of crystalline *p*TP.

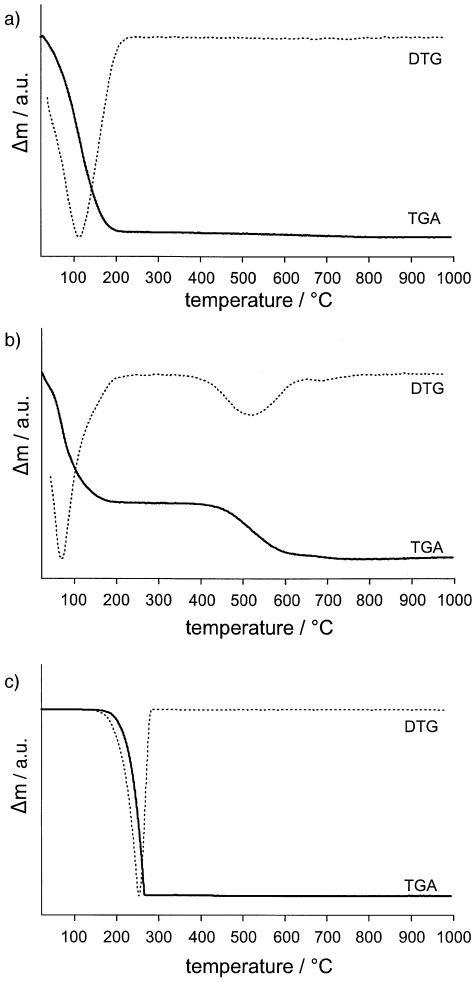

Figure 2. TGA and its first derivative (DTG) of a) hydrated zeolite L, b) wet *p*TP-zeolite L and c) crystalline *p*TP observed at a heating rate of 5 °C per min in a nitrogen stream of 15 mL per min.

Coadsorption of water and displacement reaction in *p*TP-zeolite L—Water adsorption kinetics

For the handling of dry neutral-dye zeolite L samples, it is important to know how fast and how much water is readsorbed by the sample. Figure 3a) shows the water adsorption kinetics of a dehydrated zeolite L sample, when exposed to laboratory air of 18–22 % relative humidity at rt. The initial adsorption rate of about 1 H_2O per u.c. per h remains constant until about 12 H_2O per u.c. are adsorbed and then decreases until equilibrium is reached after about 24 h. The water content at equilibrium was determined from the subsequent TGA to about 16 H_2O per u.c. Figure 3b) shows the adsorption kinetics of a dry *p*TP-zeolite L sample under the same conditions. Here, the initial adsorption rate is higher compared with Figure 3a). It decreases to a rate of about 1 H_2O per u.c. per h when about 12 H_2O per u.c. are adsorbed and then levels off. The water content at equilibrium was determined to about 16 H_2O per u.c.

The amount of water adsorbed by the two samples is identical but the adsorption kinetics are different. In the case of dry *p*TP-zeolite L two kinetic processes are observable leading to an earlier establishment of equilibrium compared with the dehydrated zeolite L case.

0947-6539/00/0618-3460 $ 17.50+.50/0 *Chem. Eur. J.* **2000**, *6*, No. 18

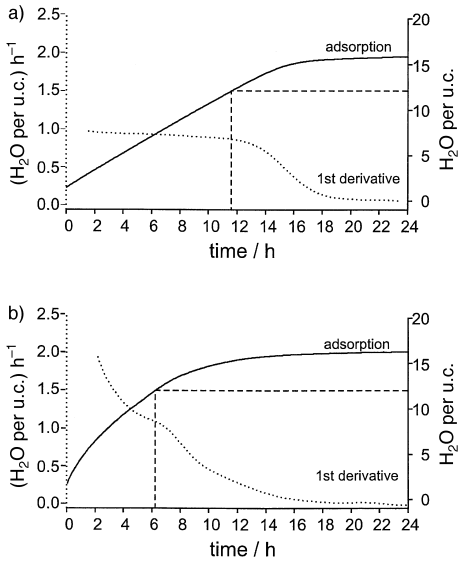

Figure 3. Water adsorption kinetics observed for a) dehydrated zeolite L and b) dry *p*TP-zeolite L at laboratory air of 18–22% rel. hum. over a time period of 24 h (solid line). The corresponding adsorption rates are displayed as dotted lines. The dashed lines indicate the changes of the adsorption rates when about 12 H_2O per u.c. are adsorbed.

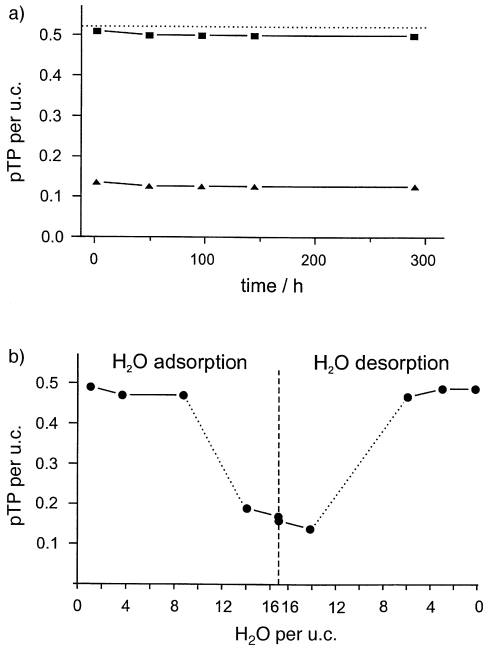

Figure 4. a) Amount of *p*TP per u.c. staying inside the zeolite, when dry *p*TP-zeolite L (squares) or wet *p*TP-zeolite L (triangles) are dispersed in 1-butanol. The total amount of *p*TP per u.c. contained in the sample after the synthesis is indicated as dotted line. b) Amount of *p*TP per u.c. located inside the zeolite depending on the amount of co-adsorbed H_2O per u.c. The water content of the sample was varied either by adsorption of water through the dry *p*TP-zeolite L sample (left side) or desorption of water from a wet *p*TP-zeolite sample (right side). The dotted line indicates the region where it was difficult to get accurate data.

Influence of co-adsorbed water on the dye location: To investigate the dye location as a function of the co-adsorbed water, a method to distinguish between the dyes located inside and outside the zeolite channels was developed. Figure 4a) shows the amount of *p*TP per u.c. located inside the zeolite as a function of time, when suspended in 1-butanol. It was determined by comparing the amount of *p*TP in the 1-butanol phase with the total amount in the sample. In the case of a dry *p*TP-zeolite L (squares), only about 5% of the *p*TP was dissolved immediately in 1-butanol. Over a period of at least 300 h the amount of *p*TP located in the channels was observed to be constant at 0.5 *p*TP per u.c., which corresponds to an occupation probability *p* of 1.

When the dry *p*TP-zeolite L is first equilibrated with water vapor of 22% relative humidity at rt and then suspended in 1-butanol (triangles), about 75% of the *p*TP can be found in the solvent after some minutes and only 0.13 *p*TP per u.c. remain in the zeolite. This situation is stable over a period of at least 300 h. The immediate dissolution of *p*TP can be attributed to molecules located at the outer surface of the zeolite crystals. The stability of the *p*TP inside the zeolite L channels is due to the fact that 1-butanol does not displace *p*TP from the zeolite L channels. The washing with 1-butanol can therefore be used to selectively remove the molecules located outside of the zeolite channels. The large amount of *p*TP which can be washed off in the wet *p*TP-zeolite L sample is caused by its displacement by co-adsorbed water according to Equation (2).

The *p*TP displacement by water upon rehydration of the stable dry *p*TP-zeolite L sample was investigated in detail by controlling the amount of co-adsorbed water. Figure 4b) shows the amount of *p*TP per u.c. located inside the zeolite channels containing different amounts of co-adsorbed water. Between 1 and about 10 H_2O per u.c. almost all *p*TP is located inside the channels. Then the displacement of the *p*TP by water starts and leads to the situation of hydrated *p*TP-zeolite L already known from Figure 4a). This process is reversible. When desorbing the water again the *p*TP moves back into the channels. The location of the *p*TP can reversibly be changed according to Equation (2) by controlling the amount of co-adsorbed water through adsorption or desorption of water at temperatures between 25 °C and 200 °C. The first 8–10 H_2O per u.c. co-adsorbed do not enter into competition with the *p*TP inside the channels.

If all displaced *p*TP molecules adsorb on the zeolite outer surface, the crystals would be covered by about 30 monolayers. Other possibilities are the formation of an isolated crystalline phase or a mixture of the two aggregation states. To get more information about the state of the *p*TP a series of experiments was carried out. A hydrated zeolite L sample was impregnated with *p*TP as described in the Experimental Section (first step of impregnation method). The *p*TP was located outside the zeolite L since its channels were filled with water. The TGA of this sample looked exactly the same as the TGA of the wet *p*TP-zeolite L shown in Figure 2b). From this, one might be tempted to conclude that the observed weight loss above 400 °C is due to desorption of *p*TP from the outer surface because crystalline *p*TP would desorb around 250 °C (see Figure 2c)). However, this conclusion is wrong. For a better understanding of what is going on in the sample during the TGA measurement, different samples of wet *p*TP-zeolite L and of *p*TP-impregnated zeolite L were partially dehydrated in the thermobalance by heating under TGA conditions from 25 to 220 °C. The total weight loss in this

  0947-6539/00/0618-3461 $ 17.50+.50/0

temperature interval was 10.0% by weight for all samples. The same amount of water was desorbed in the case of hydrated zeolite L in this interval. The dehydration was therefore completed to 95% corresponding to 1 H_2O per u.c. remaining in the zeolite. The washing of this partially dehydrated samples with 1-butanol showed that only about 3% of the total amount of *p*TP present could be removed. This means that during the dehydration a subsequent insertion of the *p*TP into the zeolite channels takes place in both samples. This corresponds to the same process as reported in Figure 4b). The desorption processes seen in the TGA above 220 °C are therefore due to desorption of *p*TP or reaction products located inside the zeolite L channels.

Raman spectra of *p*TP samples

Raman spectroscopy is a powerful tool for the investigation of structural integrity of dye-loaded zeolite samples and of host–guest interactions. In Figure 5 (1) the Raman spectrum of hydrated zeolite L is shown. The peaks at 498 cm^{-1}, 605 cm^{-1}, and the flat band at 1140 cm^{-1} were already described by Angell.[45] The first one can be assigned to the symmetric bending vibration (the O atom moves along the

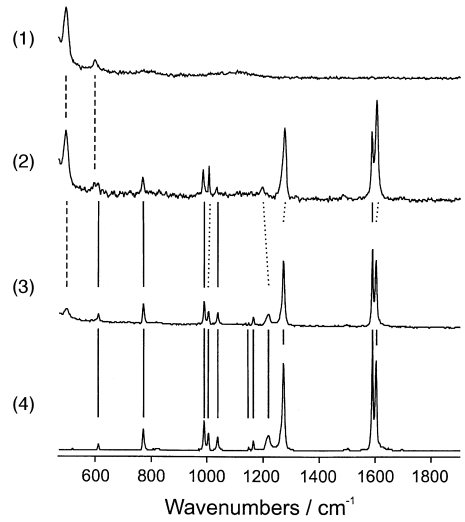

Figure 5. Raman spectra of (1) hydrated zeolite L, (2) dry *p*TP-zeolite L, (3) wet *p*TP-zeolite L and (4) crystalline *p*TP. Spectra (2) to (4) are normalized to the band at 772 cm^{-1}. Spectrum (1) is normalized to the same heigth at 498 cm^{-1} relative to spectrum (2).

bisecting line of the T-O-T angle, where T represents either Si or Al). It appears to be the most structure-sensitive band.[46–50] The zeolite L bands remained unchanged upon dehydration or treatment of the zeolite L up to 1000 °C in the TGA experiments. This indicates that the framework was stable under all conditions mentioned in this paper. The dashed lines connect the corresponding zeolite L peaks appearing in the spectra of *p*TP-zeolite L. To check whether thermal decomposition of the *p*TP took place during the sample synthesis, Raman spectra of dry and wet *p*TP-zeolite L were recorded and compared with the reference spectrum of crystalline *p*TP. The conformity of the *p*TP peaks in the reference spectrum of crystalline *p*TP (4) and of wet *p*TP-zeolite L (3) shows that no decomposition of the *p*TP can be observed after the sample synthesis. Compared with the wet *p*TP-zeolite L, the spectrum of dry *p*TP-zeolite L (2) shows an increase of the zeolite peak intensities with respect to those of *p*TP. The spectral shifts of some *p*TP vibrations, are indicated by dotted lines. The peak at 1274 cm^{-1}, which can be assigned to the inter-ring stretching vibration (in analogy to the biphenyl[51]), is shifted to higher frequencies by 7 cm^{-1}. The peak at 1605 cm^{-1} is also slightly shifted to 1609 cm^{-1} and the relative intensity with respect to the 1591 cm^{-1} band changes. Peaks around 1600 cm^{-1} are typical for aromatic compounds and correspond to carbon–carbon stretch vibrations. The changes of position and intensity of the bands observed mainly in the dry *p*TP-zeolite L samples reflect the interaction of the *p*TP with the zeolite environment, which was not further analyzed.

Other neutral-dye zeolite L materials

To outline the general character of the synthesis and characterization methods, some results obtained with other neutral dyes are summarized in this Section. The characteristics of these systems also helps to improve our understanding of the host–guest interactions and the important parameters of insertion reactions. The neutral molecules shown in Scheme 1 were successfully inserted into zeolite L either by the double or the simple ampoule method at temperatures between 100 °C and 300 °C.

In the case of BP, a loading of about 1 BP per u.c. was achieved using either the simple or the double ampoule method at a temperature of 300 °C. From the high loading we infer that the BP molecule is not aligned along the zeolite L *c* axis. In other aspects the BP-zeolite L behaves similar to the *p*TP-zeolite L. Displacement by water takes place and the TGA also shows two distinct desorption steps at high temperature which are even more pronounced. The second desorption step could be due to desorption of polycondensation products formed at high temperatures, which is a typical reaction known for this class of substances.[41] The radical hydroxy-TEMPO was inserted by the double ampoule method at a temperature of 120 °C and a loading of about 1 hydroxy-TEMPO per u.c. was achieved. Displacement by water was not observed. Resorufin was introduced in its neutral form by the simple ampoule method and afterwards deprotonated inside the zeolite by treatment with ethanolic KOH solution. The displacement kinetics of resorufin anion by different molecules (water, methanol, ethanol, 1-propanol, 1-butanol) was studied in detail.[16] MBOXE was inserted using either the simple or the double ampoule method at a temperature of 170 °C. It was displaced by co-adsorbed water in a similar way as reported for *p*TP-zeolite L upon rehydration of the dry MBOXE-zeolite L, but with a slower rate. DPH could not be inserted into the zeolite by the double ampoule method because degradation started at its sublimation temperature. Therefore the simple ampoule method was used involving the insertion from the melt at 180 °C. After 30 min a butanolic solution of DPH was completely degraded (when stored in daylight) forming species absorbing in the UV (probably oxidation products). However, practically no degradation by light was observed once the DPH was inserted in the zeolite; this demonstrates the stabilizing effect of the

  0947-6539/00/0618-3462 $ 17.50+.50/0 *Chem. Eur. J.* **2000**, *6*, No. 18

zeolite host. When washing dry DPH-zeolite L with 1-butanol after the synthesis, only about 5% of the total DPH (determined from the TGA) was found in the solvent. The same amount was found for the wet DPH-zeolite L after exposure to humidity, thus indicating that water does not displace DPH. For this reason DPH was our favorite for the synthesis of the first three-dye zeolite L sandwich structure. In Figure 6a) we show the Raman spectra of hydrated zeolite L (1), of wet DPH-zeolite L (2) and of crystalline DPH (3). In the spectrum of wet DPH-zeolite L the zeolite L peaks can be observed (dashed lines). The vibrations of the DPH in the zeolite do not shift with respect to the crystalline phase with exception of the aromatic carbon–carbon stretching modes

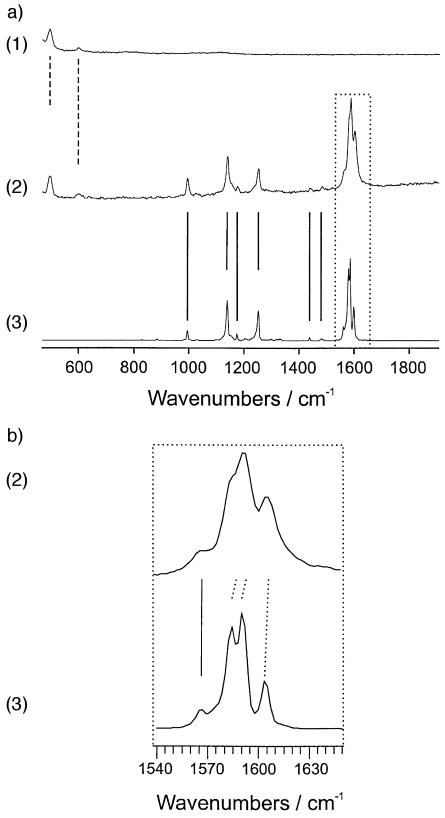

Figure 6. a) Raman spectra of (1) hydrated zeolite L, (2) wet DPH-zeolite L and (3) crystalline DPH. b) Enlargement of the peaks around 1600 cm^{-1} of (2) and (3). Spectra (2) and (3) are normalized to the band at 1142 cm^{-1}. Spectrum (1) is normalized to the same heigth at 498 cm^{-1} relative to spectrum (2).

around 1600 cm^{-1}. Figure 6b) shows an enlargement of this region. The broadening of the peaks is accompanied by minor spectral shifts of about 3 cm^{-1}, indicating an interaction of the molecule with the environment in the zeolite L channels.

Three-dye zeolite L sandwiches

Synthesis: We found that neutral dye-zeolite L materials with an occupation p smaller than one and sufficiently slow displacement kinetics can be modified with Py and Ox by means of ion exchange, according to Equation (3). This led to the discovery of the first bi-directional three-dye zeolite L antenna material. Under the fluorescence microscope the sandwich structure of single Ox,Py,DPH-zeolite L crystals can be observed by selectively filtering the DPH, Py or Ox emission. Following the same procedure as described for Ox,Py,DPH-zeolite L the system Ox,Py,MBOXE-zeolite L was also prepared and analyzed. This was possible despite the fact that MBOXE can be displaced by water, because the initial step of the exchange kinetic with Py is fast enough.

Energy migration and energy transfer experiments: We have studied the fluorescence spectra of the following materials coated as thin layers on quartz plates: DPH-zeolite L, Py-zeolite L, Ox-zeolite L, Py,DPH-zeolite L, Ox,DPH-zeolite L and Ox,Py,DPH-zeolite L. The occupation probabilities of the different dyes was the same in all the samples, namely $p_{DPH} \approx 0.50$, $p_{Py} \approx 0.10$ and $p_{Ox} \approx 0.02$. An additional Ox,Py,DPH-sample with $p_{Py} \approx 0.05$ was investigated. The Ox,Py,DPH-zeolite L sample is a deeply violet colored material.

In Figure 7a) we compare the emission spectra of DPH-zeolite L, Py-zeolite L, and Py,DPH-zeolite L, when excited at 353 nm, where the extinction coefficient of DPH is much bigger than that of Py (see Figure 1a)). We observe that the emission of the DPH-zeolite L (dotted line) has much higher intensity than the Py-zeolite L (dashed line), as expected from the higher extinction coefficient and the five times higher loading. We should add that the fluorescence quantum yield of Py and Ox in zeolite L are close to one, while we estimate that of the DPH in zeolite L to be in the order of 0.2.[52] The reference spectrum of Py-zeolite L represents the part of the Py fluorescence coming from direct excitation by the 353 nm light and the spectrum of DPH-zeolite L represents the fluorescence of DPH in absence of energy transfer. An interesting observation can be made for the Py,DPH-zeolite L (solid line). The DPH emission is reduced significantly with respect to the DPH-zeolite L and the Py emission has gained intensity. Our explanation of this observation is that energy absorbed by DPH is transferred to Py in a similar way as was reported recently for the bi-directional Py,Ox-zeolite L antenna material.[10] This observation encouraged us to prepare and investigate Ox,Py,DPH-zeolite L sandwiches in order to find out if near UV excitation of DPH, located in the middle part of the crystals, can travel all the way through the Py containing region and end up as red light emitted by Ox. The result of such an experiment is illustrated in Figure 7b), where we compare the fluorescence observed when Ox-zeolite L (dashed), Ox,DPH-zeolite L (dotted) and Ox,Py,DPH-zeolite L (solid) layers on quartz are excited at 353 nm. We observe only a weak Ox emission in case of the Ox-zeolite L sample. This was expected since Ox absorbs very weakly at 353 nm and its loading is low. The DPH fluorescence intensity of the Ox,DPH-zeolite L is quite intense and the Ox emission has also increased significantly. The energy transfer from the DPH to the Ox is responsible for this behavior, as will be explained later. The most interesting observation is made in the case of the Ox,Py,DPH-zeolite L. We see that the DPH intensity decreases with respect to the Ox,DPH-zeolite L sample and that instead of it a Py emission is build up, as already observed above. In addition to this the Ox emission intensity has increased significantly. Our interpretation for this observation is that the Py emission and the enhanced Ox

emission are due to the antenna function of the system. The energy is transferred from the electronically excited DPH to Py which either relaxes by emitting a photon or allows the energy to migrate to the boundary of the Ox domain. After energy transfer to Ox, emission of red light due to fluorescing Ox can be observed. This interpretation is supported by the excitation spectra of two Ox,Py,DPH-zeolite L samples with different Py loading, reported in Figure 7c). The two spectra were recorded at 620 nm, the emission maximum of Ox. They have been scaled to the same height at 600 nm. We observe that both spectra show features of the absorption spectra of the three dyes (see Figure 1a)), which indicates that the observed fluorescence at 620 nm can be measured when either DPH, Py or Ox molecules are excited by the light. We also observe the expected decrease of the Py intensity for the sample with half of the Py loading.

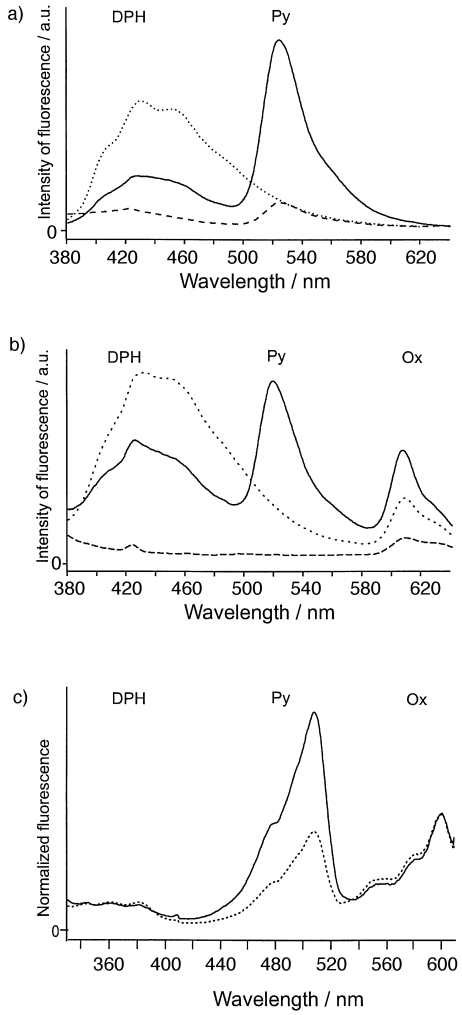

Figure 7. All spectra were recorded from thin layers on quartz plates. The occupation probabilities of the different molecules in these samples are: $p_{DPH} \approx 0.50$, $p_{Py} \approx 0.10$, $p_{Ox} \approx 0.02$. a) Comparison of the emission spectrum of Py,DPH-zeolite L (solid line) with DPH-zeolite L (dotted line) and Py-zeolite L (dashed line) as reference, when excited at 353 nm. b) Comparison of the emission spectrum of Ox,Py,DPH-zeolite L (solid line), of Ox-zeolite L (dashed line) and of Ox,DPH-zeolite L (dotted line) when excited at 353 nm. c) Excitation spectra of two Ox,Py,DPH-zeolite L samples with different Py loading recorded at 620 nm, scaled to the same hight at 600 nm. The first sample has the same composition as the one in b) (solid). The second sample has a two times lower Py loading (dotted line).

Discussion

A set of experimental tools for the synthesis and characterization of neutral dye-zeolite L materials has been reported and applied to the dyes summarized in Scheme 1. We now outline some general features of these tools and implications of the displacement reaction [Eq. (2)]. In the discussion of the three-dye zeolite L sandwiches the emphasis is on their bidirectional antenna behavior.

Insertion of neutral dyes into zeolite L: The *double ampoule method* leads to homogeneous and reproducible samples of highly dye loaded zeolite L. The handling of the materials is easy and does not require complicated equipment. Because of electrostatic effects it is difficult to weigh the dry zeolite in a glove box. It is much easier to weigh the hydrated zeolite and to dehydrate it afterwards. Therefore precisely known amounts of dye and dry zeolite can be used in this method for quantitative experiments. The glass spiral and the rotation of the ampoule provide an effective homogenization of the reaction mixture. The final material is obtained in a sealed ampoule. The *simple ampoule method* leads to comparable results. It requires the handling of the sample in the glove box. The insertion temperature is lower compared with the double ampoule procedure because insertion takes place from the melt and not from the gas phase. The *surface impregnation method* consists of simultaneous dehydration of the zeolite and insertion of the organic molecule. It leads to the same results as the two methods mentioned above in the case of *p*TP-zeolite L. It can be used for inserting less stable molecules with low partial pressures. The dehydration conditions should be chosen so that a sufficient amount of H_2O can escape the zeolite framework and a high mobility of the molecules adsorbed on the surface is guaranteed. A temperature of 200 °C and a continuous nitrogen stream led to the desired results. Obviously the mobility of the *p*TP on the zeolite surface and in the channels was high enough under these conditions. Milder conditions could be achieved by replacing the nitrogen stream with an evacuated system.

The vapor phase impregnation method described by Davis et al.[31] does need dehydration of the zeolite prior to mechanical mixing with the organic molecules. It has for example been used for the "ship in the bottle" synthesis of $Ru(bpy)_3^{2+}$ in zeolite Y.[14] It is less convenient for quantitative experiments. Procedures were neutral molecules are inserted from solution have so far not been successful for our purposes. Inclusion of dyes during the zeolite synthesis does not allow the synthesis of the sandwich structures envisaged and was therefore not considered.

A wide variety of dehydration methods have been reported in the literature. In most cases the effectiveness of the procedures were not discussed. Specific surface area measurements, TGA and gravimetric measurements represent good and simple tools to check the effectiveness of a method. We have shown that the dehydration method applied in this study leads to water free main channels of zeolite L. About 1 H_2O per u.c. still remains in the smaller side channels, which does not affect our experiments.

0947-6539/00/0618-3464 $ 17.50+.50/0 *Chem. Eur. J.* **2000**, *6*, No. 18

TGA was found to be an ideal method for determining the total *p*TP content in any *p*TP-zeolite sample. When using TGA for the analysis of other dye-zeolite samples, complications can arise such as room temperature sublimation, thermal reactions leading to polymers and other unwanted processes. Therefore the data has to be carefully interpreted when working with new classes of substances. When using TGA as the only evidence for the successful insertion of a molecule during the preparation, one has to be careful because insertion can also be a result of the processes taking place during the TGA measurements.[31]

The washing of dry dye-zeolite L materials with 1-butanol, which was first studied for resorufin-zeolite L,[16] allows us to distinguish between dyes located inside and outside of the channels. It was also used to remove molecules from the outer surface of the crystals, which is necessary when preparing sandwich structures with defined domains.

Coadsorption of water and displacement reaction: Exposure of a dry *p*TP-zeolite L to air of 22% relative humidity at rt leads to the water adsorption kinetics shown in Figure 3b). The adsorption behavior can be interpreted as a superimposition of two processes. One process dominates the first 4–6 h where the large initial rate tends asymptotically to a value of about 1 H_2O per u.c. per h. After the adsorption of 10–12 H_2O per u.c. the second process takes over and the rate slows down steadily until equilibrium is reached after about 24 h. The total capacity for water adsorption is about the same as for a dehydrated zeolite L. We have no explanation for the astonishing observation that the initial water adsorption rate of the *p*TP-zeolite L is larger than that of an unloaded sample. However, the characteristic behavior of this process can be compared with the results reported in Figure 4b). We observed that the first 10 H_2O per u.c. do not displace the inserted *p*TP. Replacement of the *p*TP by water occurs only after this limit has been exceeded. From this we know that *p*TP-zeolite L samples can easily be manipulated despite the fact that the initial water uptake is fast. The reason why the first 10 H_2O per u.c. do not displace *p*TP can be understood from the fact that at the beginning most of the cations in the dry *p*TP-zeolite L channels are free to coordinate the entering water molecules without disturbing the *p*TP. About 0.13 *p*TP per u.c. remain in the channels of the zeolite at equilibrium. This corresponds to an equivalent volume of about 0.3 H_2O per u.c. as can be estimated from the density of crystalline *p*TP (1.234 $g\,cm^{-3}$, 25 °C) and the specific volume of adsorbed water in zeolite L at rt (784 $Å^3$ per u.c.[39, 53]). This explains why the total capacity for water adsorption of the *p*TP-zeolite L was found to be the same as for an unloaded zeolite L.

The amount of *p*TP leaving a dry *p*TP-zeolite L upon exposure to humidity corresponds to an equivalent of about 30 *p*TP monolayers at the outer surface of the zeolite crystals. The *p*TP Raman spectrum of such samples is the same as that of pure crystalline *p*TP. In their TGA characteristics however, the desorption step of a crystalline *p*TP phase at 250 °C is missing. This is explained by the observation that the *p*TP, which melts at 210 °C, prefers to return into the water-free zeolite L main channels before the desorption temperature of the crystalline phase is attained. The surface impregnation method as a synthetic tool was developed based on this observation. Figure 4b) indicates how the distribution of the *p*TP between the inner and the outer surface of the zeolite crystals can be controlled. A similar observation was made by Ramamurthy et al. when studying the behavior of some ketones in zeolite Y.[34]

The fact that water can displace BP, *p*TP, Res, and MBOXE at room temperature but not for example DPH reflects different interactions of these molecules with the zeolite framework. The shape of the zeolite L main channel makes it easy for the flexible DPH to come into close contact with the wall but difficult for example for the *p*TP. More quantitative thermodynamic, kinetic, spectroscopic, and theoretical studies of this aspect for a large range of molecules would be desirable.

Three-dye sandwiches: Zeolite L permits insertion of neutral dyes [Eq. (1)] and insertion of cationic dyes by ion exchange [Eq. (3)]. This is a specific feature with respect to the popular covalent $AlPO_4$-5 and similar materials. It allowed us to design the synthesis procedure illustrated in Scheme 3 which leads to sandwich materials. Each step can either be an insertion of a neutral dye or an ion exchange with a cationic dye. If their size and shape are properly chosen, the molecules cannot glide past each other because the channels are too narrow. This allows the filling of specific parts of the nanocrystals with the desired type of molecules. We envisaged two systems. In one of them DPH, and in the other MBOXE was inserted in the first step. The amount of dye was chosen so that about 50% of the sites remained empty. In the next step Py was inserted by ion exchange. The rate of this ion exchange is fast enough at the beginning so that MBOXE does not have sufficient time to be significantly displaced by water. The dye molecules, which are further inside, have no chance to escape, as soon as one Py has been inserted on both sides of a channel. Instead they are pushed deeper in the channel by newly entering Py cations. In a next step Ox is added on each side of the channels in a similar procedure. This process could be continued, to also include neutral molecules after an ion-exchange step. This means that the procedure explained in Scheme 3 is very versatile. The high degree of organization realized in the three-dye zeolite L sandwich material is of general interest. The zeolite L host can be used to organize other molecules in a sandwich structure and to prepare materials with remarkable new properties.

Energy migration and energy transfer in 2 and 3-dye zeolite L sandwiches: Organic dyes have the tendency to form aggregates in solution even at low concentration. Such aggregates are known to cause fast thermal relaxation of the electronically excited states. The role of zeolite L in this study is to prevent this aggregation and to superimpose a specific organization. We have observed that a portion of the near UV light absorbed by the DPH, which is located in the middle part of the Ox,Py,DPH-zeolite L nanocrystals, is transferred to the adjacent Py, travels all the way through the Py containing section and is then transferred to the Ox located at both ends of the crystals, where it is emitted as red light.

Similar observations have been made with Ox,Py,MBOXE-zeolite L materials.

Energy transfer and migration in these systems are governed by dipole–dipole interactions known as Förster mechanism[54] due to the absence of any orbital overlap between the dye molecules. Consequences of Förster's energy transfer in such materials have been reported in a theoretical study.[19] It turned out that it is convenient to express the rate constant for energy transfer from a donor *i* to an acceptor *j* as follows:

$$k_{ij} = \frac{9\ln(10)\phi_i}{128\pi^5 N_A n^4 \tau_i} G_{ij} J_{ij} p_i p_j \quad (5)$$

where ϕ_i and τ_i [s^{-1}] are the fluorescence quantum yield and the intrinsic fluorescence lifetime of the donor, N_A [mol^{-1}] is Avogadro number, n is the refractive index of the medium, G_{ij} [$Å^{-6}$] expresses the geometrical constraints of the sites in the crystal and the relative ordering of the electronic transition moments, p_i and p_j are the occupation probabilities of the sites with excited donors *i* and acceptors *j* in the groundstate, and J_{ij} [$cm^3 M^{-1}$] is the spectral overlap integral between the donor emission and the acceptor absorption spectrum. The energy migration rate constant k_i^E is obtained by summing up the individual k_{ij} for the energy migration between an excited donor and all surrounding acceptors:

$$k_i^E = \sum_{j \neq i} k_{ij} \quad (6)$$

Spontaneous fluorescence, internal conversion and intersystem crossing compete with the energy transfer and energy migration processes as indicated in Scheme 4. The depopulation rate of an excited donor *i* can be expressed according to Equation (21) of ref. [19] by:

$$k_i = k_F + k_{tr} + k_i^E + \sum_J k_{ij}$$

where k_F is the intrinsic fluorescence rate constant, k_{tr} is the rate constant of thermal relaxation including internal conversion and intersystem crossing, and the k_{iJ} are the rate constants for energy transfer from a donor *i* to an acceptor *j* at the domain boundary. Quantitative evaluation of for example front–back trapping efficiencies can be made in a similar way as described in ref. [19] but is considerably more complex. We

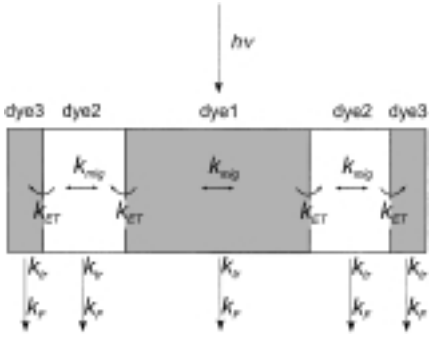

Scheme 4. Three-dye zeolite L sandwich crystal and photophysical processes occurring after excitation of dye1: energy migration (k_{mig}), energy transfer (k_{ET}), thermal relaxation including internal conversion and intersystem crossing (k_{tr}), spontaneous fluorescence (k_F).

observed in our recently published study on Ox,Py-zeolite L significantly larger energy migration length than predicted by Förster energy migration.[10] Our data strongly indicates that this is due to self-absorption and re-emission processes, causing a longer effective fluorescence lifetime.[9]

Instead of trying a quantitative account on the antenna properties of the Ox,Py,DPH-zeolite L and Ox,Py,MBOXE-zeolite L materials for which we are not yet ready, some qualitative arguments are useful. After selective excitation of a dye1 located in the middle part of a dye3,dye2,dye1-zeolite L successive energy migration steps take place until the phase boundary dye2,dye1 has been reached, where energy transfer to dye2 can take place. This step is not reversible because a portion of the excitation energy is lost. The remaining exitation energy then migrates to the next phase boundary dye3,dye2 where the same process can happen. Dye3 finally relaxes to its groundstate either by fluorescence or by a radiationless processes. The rate constants for the energy migration and transfer are directly proportional to the spectral overlap J_{ij} which are illustrated qualitatively in Figure 8 for DPH, Py and Ox as shaded areas.

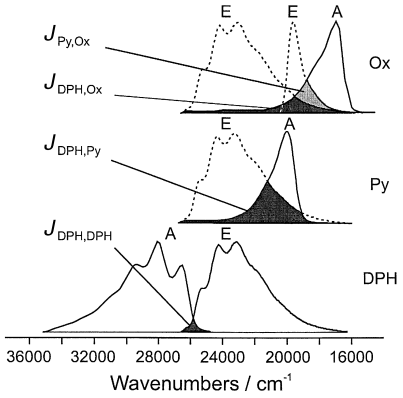

Figure 8. Bottom: Absorption (A) and emission spectrum (E) of DPH. The shaded area indicates the DPH/DPH spectral overlap. Middle: Emission spectrum of DPH and absorption spectrum of Py. The dark area indicates the DPH/Py spectral overlap. Top: Emission spectra of DPH and Py and absorption spectrum of Ox. The DHP/Ox and the Py/Ox spectral overlap integrals are indicated.

We first discuss the consequences for energy migration. Based on the spectral overlap, the fluorescence quantum yield and lifetime, energy migration is fastest in Ox, followed by Py. It is slower in DPH and MBOXE. Since G_{ij} is an intrinsic constant in the case of energy migration, the important parameter that can be varied is the occupation probability. The occupation probabilities which apply here can only be estimated. The values given for the Ox,Py,DPH-zeolite L material in the section on the synthesis of three-dye zeolite L sandwiches refer to a whole micro crystal. Since the DPH, which is initially inserted, is first compressed by the following Py and then also by the following Ox, we must now use the "local p_{DPH}" which is larger than 0.5. By similar reasoning we know that the "local p_{Py}" is larger than 0.1 and that "local p_{Ox}" is larger than 0.02. More quantitative knowledge of the "local" occupation probability is not available but would be desirable, which means that new analytical techniques are

0947-6539/00/0618-3466 $ 17.50+.50/0 *Chem. Eur. J.* **2000**, *6*, No. 18

needed. For energy transfer, the G_{ij} is no longer an intrinsic parameter only determined by the crystal symmetry and the relative orientation of the electronic transition moments. It must be expressed specifically at each of the four dye*i*,dye*j* boundaries. The probability that DPH can transfer its energy in an Ox,Py,DPH-zeolite L crystal directly to Ox is small because of the Py layer located between them, which makes the DPH to Ox distance much too long to compete with the DPH to Py energy transfer. In a Ox,DPH-zeolite L material, however, some DPH to Ox energy transfer is possible because of the shorter distance and the non vanishing $J_{DPH,Ox}$ spectral overlap. This explains the increase of the Ox emission illustrated in Figure 7b).

The efficiency of DPH excitation energy transport to Ox depends strongly on the energy migration length l_{DPH} in the DPH region located in the middle part of the cylinders and on l_{Py}. The length of the DPH region can be estimated to be more than 400 nm, which means that severe losses are to be expected due to the relatively low fluorescence quantum yield of DPH. This is supported by the excitation spectra shown in Figure 7c), observed at the Ox emission maximum. The absorption characteristics of all three dyes can clearly be recognized and we conclude that Ox can be excited at each wavelength shown, ranging from 330 to 620 nm, in both cases. The part of the Ox emission caused by light absorption of the DPH at 353 nm is smaller than the emission due to the direct Py excitation at 495 nm. The distribution of excited Py in the zeolite is completely different in the case of direct light absorption compared with the case of excitation by energy transfer from the DPH. In the first case the whole Py domain is excited homogeneously, while in the second case only Py near the Py,DPH boundary can be excited. The Py intensity shown in Figure 7c) differs by a factor of about two as expected for the different Py loading. Interestingly the relative intensity of the Ox to DPH fluorescence is the same in both spectra. This means that the loss in the Py energy transfer rate is not the determining step for the DPH → Py → Ox excitation energy transport. We conclude that a significant amount of excitation energy is lost within the DPH region because the energy migration length is significantly shorter than the length of the DPH section and a large part of the DPH domain does not contribute to the energy transfer. A dye with a significantly larger fluorescence quantum yield but otherwise similar characteristics as DPH is therefore expected to show a larger energy transport efficiency. In Figure 9 we report the results of a similar experiments to those shown in Figure 7b) and c), except in this case for the Ox,Py,MBOXE-zeolite L material. We observe that the Ox fluorescence in Figure 9a) is now even more intense with respect to the Py emission. The absorption characteristics of MBOXE in the excitation spectrum b) is comparable in intensity to the Ox contribution.

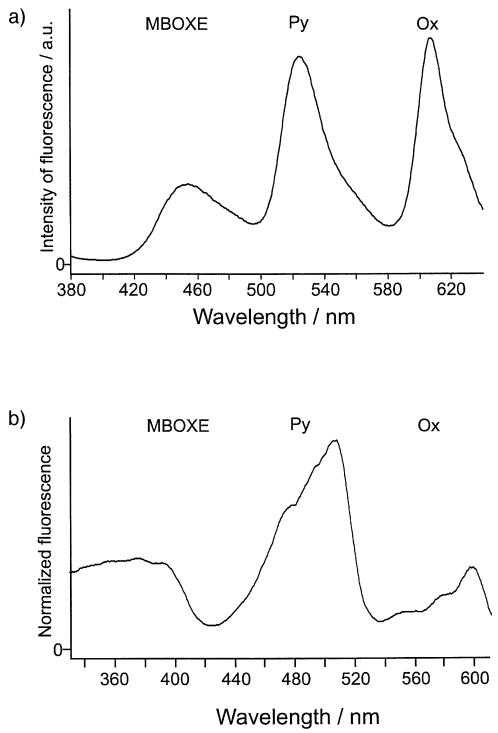

Figure 9. a) Emission spectrum of Ox,Py,MBOXE-zeolite L when excited at 364 nm. b) Excitation spectrum of Ox,Py,MBOXE-zeolite L recorded at 627 nm.

Conclusion

A new kind of artificial antenna systems with light harvesting properties over the whole visible spectrum and effective energy transfer was demonstrated on two different materials. The concept described for preparing and characterizing dye loaded zeolite L sandwich structured material is not limited to the dyes reported in Scheme 1 and it is not limited to zeolite L. Optimization of the energy transport efficiency is possible and we are confident that the linking of these antenna systems to appropriate molecular or extended acceptors will lead to devices with fascinating properties.

Experimental Section

Physical measurements: UV/Vis spectra were recorded on a Lambda 14 spectrophotometer (Perkin–Elmer). Fluorescence spectra were recorded on a luminescence spectrometer LS50B (Perkin–Elmer). For the fluorescence measurements of the sandwich materials and the reference samples, about 1 μm thick layers were prepared on quartz plates. The dye-loaded zeolite was suspended in 1-butanol (1.5 mL). 200 µL of this suspension were put as droplet on a quartz plate (1.5 cm diameter) and covered by a petri dish top. After 4–6 h the solvent was evaporated and the layers were ready for the measurements. FT-Raman measurements were performed with the Raman accessory of a BOMEM DA3.01 FTIR spectrometer, equipped with quartz beamsplitter and a liquid nitrogen cooled InGaAs-detector. The excitation wavelength of 9394.5 cm^{-1} was generated by a cw-Nd^{3+}:YAG Laser (Quantronix Model 114). The samples were filled in glass tubes (DURAN, inner diameter 1.6 mm) and sealed afterwards (the dry dye-zeolite L samples were handled in the glove box). The spectra were recorded with a laser power between 250 and 390 mW, a resolution of 4 cm^{-1} and 1000 scans. Specific surface area measurements were made on a Sorptomatic 1990 instrument (including Krypton unit from CE-Instruments) using argon as adsorbate at ≈87 K in the range of relative partial pressures p/p_0 from 10^{-4} to 1. Thermo gravimetric analysis (TGA) and water adsorption kinetics were measured on a Mettler Thermobalance TG50. For the water adsorption kinetics experiment the thermobalance was exposed to laboratory air with a relative humidity of 18–22 % and the temperature was held constant at 25 °C. Filtering of zeolite suspensions was

performed with a polycarbonate membrane filter (Millipore Isopore Membrane Filter, 0.1 μm, VCTP).

Materials: *p*-Terphenyl (*p*TP) (Aldrich, 99.5 %) was used as received. The extinction coefficient was determined in 1-butanol as $\varepsilon_{(278\,nm,BuOH)} = 3.6 \times 10^4\,L\,mol^{-1}\,cm^{-1}$. all-*trans*-1,6-Diphenyl-1,3,5-hexatriene (DPH) (Fluka, > 99 % HPLC) was used as received. The extinction coefficient reported for methanol as solvent was used:[55] $\varepsilon_{(350\,nm,MeOH)} = 8.28 \times 10^4\,L\,mol^{-1}\,cm^{-1}$. The extinction coefficient of 1,2-bis(5-methyl-benzoxazol-2-yl)-ethene (MBOXE) in ethanol was reported to be $\varepsilon_{(362\,nm,EtOH)} = 4.3 \times 10^4\,L\,mol^{-1}\,cm^{-1}$.[56] Pyronine (Py) with acetate and oxonine (Ox) with perchlorate as counter ion were synthesized and purified according to the procedures described in the literature.[26, 57, 58] The extinction coefficients of pyronine ($\varepsilon_{max} = 8.3 \times 10^4\,L\,mol^{-1}\,cm^{-1}$) reported by Müller[57] and oxonine ($\varepsilon_{max} = 7.8 \times 10^4\,L\,mol^{-1}\,cm^{-1}$) reported by Vogelmann[59] were used in all subsequent measurements. The fluorescence quantum yields and the natural lifetimes of the dyes used in the sandwich materials are $\Phi_{DPH,MeOH} = 0.27/\tau_{DPH,MeOH} = 19.3$ ns,[55] $\Phi_{MBOXE,EtOH} = 0.78/\tau_{MBOXE,EtOH} = 1.5$ ns,[56] $\Phi_{Py,EtOH} \approx 1/\tau_{Py,EtOH} = 3.2$ ns,[60] $\Phi_{Ox} \approx 1/\tau_{Ox,EtOH} = 3.5$ ns.[59]

1-Butanol (Fluka, for UV spectroscopy, > 99.8 %) was used as solvent without further drying. Zeolite L was synthesized as described elsewhere.[10] Elementary analysis of a representative zeolite sample yielded the formula $K_{8.5}[Al_{8.5}Si_{27.5}O_{72.0}] \cdot nH_20$. By means of TGA the water content of the zeolite stored at 22 % relative humidity was determined by weight loss up to 1000 °C to be $n = 16.2 \pm 0.2$. The material used in the present work consisted of cylinders with an average length of about 800 nm and a diameter of 1100 nm.

Synthesis of dye-loaded zeolite L materials: Three methods for the insertion of neutral dyes into zeolite L channels are described. Most procedures are explained for *p*TP as an example, but can also be applied to other neutral dyes (see section on other neutral-dye zeolite L materials). The appropriate synthesis method was chosen depending on the dyes characteristics. In addition, the method for the synthesis of sandwich structures by modification of a neutral-dye loaded zeolite L is described.

Insertion of neutral dyes: *Double ampoule method*: The synthesis was performed in a specially designed glass ampoule. Two simple ampoules were connected at their bottom end via a thin capillary. This capillary was closed at one end by a thin glass hook, dividing the double ampoule into two cavities. In a typical experiment hydrated zeolite L (200 mg) was introduced in the left cavity and heated at 400 °C for 24 h under vacuum (3×10^{-2} mbar). After this dehydration step the left cavity of the double ampoule was sealed. *p*TP (9.5 mg) was then introduced into the other cavity. After flushing several times with N_2(g) and evacuating to a pressure of 3×10^{-2} mbar, the ampoule was cooled with liquid nitrogen to prevent sublimation of the *p*TP and sealed. The glass hook, separating the two cavities, was then broken by means of a little glass ball and insertion took place at 300 °C. A temperature gradient in the oven helped to direct the sublimation to the zeolite containing cavity. Rotation of the ampoule in the oven and a glass spiral secured a continuous homogenization of the sample. After 24 h the temperature gradient was inverted by turning the ampoule in the oven and the sample was slowly cooled to room temperature. This step secured the separation of excess dye molecules which were neither adsorbed on the outer surface nor inserted in the zeolite. The zeolite containing cavity was then cooled with liquid nitrogen and the cavities were separated by sealing the connecting capillary.

Simple ampoule method: In a typical experiment hydrated zeolite L (200 mg) was introduced in a simple ampoule (equipped with a glass spiral) and dehydrated at 400 °C at 3×10^{-2} mbar during 24 h. The sealed ampoule was opened in the glove box and *p*TP (9.5 mg) was introduced. The ampoule was then connected to the vacuum line until a pressure of 3×10^{-2} mbar was achieved. The ampoule was cooled with liquid nitrogen, sealed and rotated in the center of the oven at 300 °C. After 24 h the sample was slowly cooled to room temperature. For the gravimetric experiments hydrated zeolite L was dehydrated in a simple ampoule under the same conditions (400 °C, 24 h, 3×10^{-2} mbar) and sealed for later use.

Surface impregnation method: In a first step hydrated zeolite L (50 mg) was suspended in 1-butanol (5 mL) containing *p*TP (2.4 mg). The 1-butanol was then removed by distillation under reduced pressure at 60 °C. The remaining powder was dried at a vacuum line (3×10^{-2} mbar) for 24 h. The powder was stored at 22 % rel. hum. during 24 h before use. In a second step portions of wet sample (about 30 mg) were filled in a 1 mL ampoule and heated in a nitrogen stream of 160 mL min^{-1} at 200 °C for 3 h. Then the hot ampoule was taken out of the oven and immediately sealed.

Synthesis of dye-loaded sandwich crystals: For the synthesis of Py,DPH-zeolite L wet DPH-zeolite L (3 mg) was placed in a 10 mL test tube and suspended in water (4 mL), containing pyronine (300 μL of a 6×10^{-5} M solution). The test tube was connected to a reflux condenser and protected with aluminium foil against daylight. The suspension was refluxed for 90 min and then cooled to room temperature. After centrifugation of the suspension the solvent was decanted off. The zeolite was washed with portions of 4 mL water until no further dye was detected in the supernatant. In the same way as described for pyronine, an Ox,DPH-zeolite L sample was prepared with oxonine (40 μL of a 5.7×10^{-5} M solution) and heated under reflux for 30 min. As a reference, Py-zeolite L and Ox-zeolite L were prepared in the same way as the corresponding DPH-samples taking hydrated zeolite L (3 mg) as starting material instead of wet DPH-zeolite L.

For the synthesis of Ox,Py,DPH-zeolite L samples, the method mentioned above was applied twice. First, wet DPH-zeolite L (3 mg) was modified with pyronine as described above. After the suspension was heated under reflux 90 min, it was cooled to 70 °C and oxonine (40 μL of a 5.7×10^{-5} M solution) was added. The temperature was raised again and the suspension was refluxed for another 30 min. Then the suspension was cooled to room temperature and washed in the same way as described before. Ox,Py, MBOXE-zeolite L samples were synthesized in a similar way.

Characterization: Again we explain the different procedures in detail for *p*TP-zeolite L materials. Similar experiments were carried out with other neutral dye-zeolite L samples.

Dehydration of zeolite L and specific surface area measurements: Two methods of dehydration were used: *Dehydration at the Sorptomatic Instrument port*: Hydrated zeolite L (200 mg) was placed in a burette connected to a vacuum port and heated in an oven at a rate of 0.5 °C per min up to 300 °C. The sample was held at this temperature under dynamic vacuum conditions for 16 h until the residual pressure was $< 10^{-4}$ torr. The weight of dry zeolite L was calculated by comparing the weight of the empty degassed sample burette and the degassed sample burette containing zeolite after dehydration. The weight loss of the sample due to dehydration was in agreement with the total water content determined by TGA. *Dehydration method used in preparation technique*: The zeolite L sample was degassed in the Sorptomatic standard burette under the same conditions as used for the *p*TP-zeolite L synthesis described above (400 °C, 24 h, 3×10^{-2} mbar). For the argon adsorption measurement, the evacuated burettes were connected to the measuring port of the Sorptomatic instrument, evacuated to a pressure of $< 10^{-4}$ Torr and cooled in liquid argon. The argon adsorption isotherms of the dehydrated zeolite L samples were then collected and the specific monolayer surface areas were calculated according to the BET theory.[24]

Gravimetric determination of the water content: The water content after preparation was determined by a gravimetric method. The ampoule containing for example dry *p*TP-zeolite L was opened in a glove box and a portion of the sample (50 – 100 mg) was transferred into a glass vessel of known weight. The closed vessel was then weighed on a microbalance to determine the quantity of sample filled in. After rehydration the sample weight was determined again and the quantity of adsorbed water was calculated and compared with the total water content known from TGA measurements. The same procedure was also followed when the water content of dehydrated zeolite L was determined.

Thermo gravimetric analysis: The composition of a typical sample was determined by means of TGA. Wet *p*TP-zeolite L (15 – 30 mg) was filled into a 70 μL aluminium oxide crucible, placed in the thermobalance and heated in a N_2(g) stream of about 15 mL min^{-1} from 25 to 1000 °C with a rate of 5 °C per min. The total water content of hydrated zeolite L was determined following the same procedure.

Washing of dry and wet samples with 1-butanol: To determine the amount of dye located outside the zeolite channels and to remove it, the following washing procedure was used. In the glove box dry *p*TP-zeolite L (30 mg) was filled in a dried and weighed 50 mL bulb, equipped with magnetic stirrer and septum. 1-Butanol (30 mL) was then introduced through the septum by a syringe. The suspension was put in an ultrasonic bath for

0947-6539/00/0618-3468 $ 17.50+.50/0 *Chem. Eur. J.* **2000**, *6*, No. 18

several minutes and then portions of 5 mL were transferred to dried 10 mL test tubes equipped with magnetic stirrers. The tubes were closed by gas-tight caps and the suspensions were stirred at room temperature. After a specified time the solvent was removed by filtration of the suspension and the amount of dissolved *p*TP was determined spectrometrically. The wet *p*TP-zeolite L was washed by the same method. The same method was applied to the other dye-zeolite materials.

Coadsorption of water and displacement reaction: The water adsorption kinetics were measured on a thermobalance. Dry *p*TP-zeolite L (20–40 mg) was filled in the glove box into a 70 μL aluminium oxide crucible of known weight, transferred to the thermobalance in a sealed glass vessel and quickly put onto the balance where the weight gain at 25 °C and laboratory air (18–22 % rel. hum.) was recorded over 24 h. The same procedure was used when measuring the water adsorption kinetics of dehydrated zeolite L.

Known amounts of water were adsorbed on a dry *p*TP-zeolite L sample applying the following method: In the glove box, defined amounts of dry *p*TP-zeolite L were transferred into glass vessels of known weight. The closed vessels were then weighed on a microbalance to determine the quantity of sample filled in. The samples were exposed to 22 % rel. hum. for defined periods of time until the weight gain had reached the desired value. The amount of sample was chosen in a way that the weight gain observed was about 1 mg, independent of the relative amount of water adsorbed. The vessels were sealed and stored for 4 h at 80 °C to obtain a homogeneous distribution of the adsorbed water. The samples were washed for 24 h with 1-butanol following the washing method described above and the amount of *p*TP in the washing liquid was determined spectrometrically after filtration.

Known amounts of water were also desorbed from wet *p*TP-zeolite L samples. Defined amounts of wet *p*TP-zeolite L were filled into glass ampoules having a volume of about 1 mL. The ampoules were then placed in an oven at 100 °C (or 200 °C for high degree of dehydration) for a certain time and flushed with dry nitrogen at a rate of about 120 mL min^{-1}. The ampoules where taken out of the oven and sealed. After storage at 80 °C for 4 h the weight loss was determined. The amount of sample was chosen in a way that the weight loss observed was about 1 mg, independent of the relative amount of water desorbed. For the calculation of the exact amount of desorbed water from the sample, the water desorbed from the glass surface had to be taken into account. The samples were then washed for 24 h with 1-butanol following the washing method described above and the amount of *p*TP in the washing liquid was determined spectrometrically after filtration.

Dehydration during TGA measurement: Wet *p*TP-zeolite L (25 mg), either prepared by the double ampoule method or by the first step of the surface impregnation method, was placed in a 70 μL aluminium oxide crucible and put on the thermobalance. Then the TGA measurement was started under the same conditions as described before and the weight loss between 25 and 220 °C was monitored. At 220 °C the measurement was stopped and the sample was quickly transferred from the crucible into a 25 mL dried volumetric flask equipped with septum and magnetic stirrer. 1-Butanol (25 mL) was added and the suspension was stirred for 24 h. The solvent was separated by filtration and the amount of *p*TP contained was determined spectrometrically.

Acknowledgement

We thank Silke Megelski for the zeolite synthesis and the argon adsorption measurements and Dr. Roland Seifert for helpful discussions. This work was supported by the Swiss National Science Foundation Project NF 2000-053414/98/1 and NFP 36/4036-043853.

[1] J. M. Thomas, *Angew. Chem.* **1988**, *100*, 1735; *Angew. Chem. Int. Ed. Engl.* **1988**, *27*, 1673.
[2] J. Caro, G. Finger, E. Jahn, J. Kornatowski, F. Marlow, M. Noack, L. Werner, B. Zibrowius, *Proc. Int. Zeol. Conf. 9th* **1993**, *2*, 683.
[3] T. Bein, *Chem. Mater.* **1996**, *8*, 1636.
[4] S. D. Cox, T. E. Gier, G. D. Stucky, *Chem. Mater.* **1990**, *2*, 609.
[5] G. D. Stucky, J. E. MacDougall, *Science* **1990**, *247*, 669.
[6] D. Brühwiler, R. Seifert, G. Calzaferri, *J. Phys. Chem. B* **1999**, *103*, 6397.
[7] U. Vietze, O. Krauss, F. Laeri, G. Ihnlein, F. Schüth, B. Limburg, M. Abraham, *Phys. Rev. Lett.* **1998**, *81*, 4628.
[8] G. Calzaferri, *Chimia* **1998**, *52*, 525.
[9] G. Calzaferri, D. Brühwiler, S. Megelski, M. Pfenniger, M. Pauchard, B. Hennessy, H. Maas, A. Devaux, U. Graf, *Solid State Sci.* **2000**, *2*, 241.
[10] N. Gfeller, S. Megelski, G. Calzaferri, *J. Phys. Chem. B* **1999**, *103*, 1250.
[11] D. Wöhrle, G. Schulz-Ekloff, *Adv. Mater.* **1994**, *6*, 875.
[12] F. Schüth, *Chem. uns. Zeit* **1995**, *29*, 45.
[13] G. A. Ozin, A. Kuperman, A. Stein, *Angew. Chem.* **1989**, *101*, 373; *Angew. Chem. Int. Ed. Engl.* **1989**, *28*, 359.
[14] P. Lainé, M. Lanz, G. Calzaferri, *Inorg. Chem.* **1996**, *35*, 3514.
[15] R. Seifert, A. Kunzmann, G. Calzaferri, *Angew. Chem.* **1998**, *110*, 1604; *Angew. Chem. Int. Ed.* **1998**, *37*, 1521.
[16] D. Brühwiler, N. Gfeller, G. Calzaferri, *J. Phys. Chem. B* **1998**, *102*, 2923.
[17] V. Ramamurthy, D. R. Sanderson, D. F. Eaton, *J. Am. Chem. Soc.* **1993**, *115*, 10438.
[18] N. Gfeller, S. Megelski, G. Calzaferri, *J. Phys. Chem. B* **1998**, *102*, 2433.
[19] N. Gfeller, G. Calzaferri, *J. Phys. Chem. B* **1997**, *101*, 1396.
[20] D. W. Breck, *Zeolite Molecular Sieves*, *Structure*, *Chemistry and Use*, Wiley, New York, **1972**.
[21] D. Barthomeuf, *J. Phys. Chem.* **1979**, *83*, 249.
[22] E. M. Flanigen, *Zeolite Chemistry and Catalysis*, *ACS Monograph 171* (Ed.: J. A. Rabo), **1976**, p. 80.
[23] B. Müller, G. Calzaferri, *J. Chem. Soc. Faraday Trans.* **1996**, *92*, 1633.
[24] B. Hennessy, S. Megelski, C. Marcolli, V. Shklover, C. Bärlocher, G. Calzaferri, *J. Phys. Chem. B* **1999**, *103*, 3340.
[25] G. Calzaferri, N. Gfeller, *J. Phys. Chem.* **1992**, *96*, 3428.
[26] F. Binder, G. Calzaferri, N. Gfeller, *Proc. Ind. Acad. Sci. Chem. Sci.* **1995**, *107*, 753.
[27] C. Dybowski, *J. Inclusion Phenom. Mol. Recognit. Chem.* **1995**, *21*, 113.
[28] J. M. Newsam, *J. Phys. Chem.* **1989**, *93*, 7689.
[29] M. Malinowski, S. Malinowski, S. Krzyzanowski, *J. Therm. Anal.* **1976**, *10*, 339.
[30] K.-K. Iu, J. K. Thomas, *Langmuir* **1990**, *6*, 471.
[31] S. B. Hong, H. M. Cho, M. E. Davis, *J. Phys. Chem.* **1993**, *97*, 1622.
[32] S. B. Hong, H. M. Cho, M. E. Davis, *J. Phys. Chem.* **1993**, *97*, 1629.
[33] V. Ramamurthy, D. R. Sanderson, D. F. Eaton, *J. Phys. Chem.* **1993**, *97*, 13380.
[34] Z. Zhang, N. J. Turro, L. Johnston, V. Ramamurthy, *Tetrahedron Lett.* **1996**, *37*, 4861.
[35] K. B. Yoon, T. J. Huh, J. K. Kochi, *J. Phys. Chem.* **1995**, *99*, 7042.
[36] R. M. Barrer, H. Villiger, *Z. Kristallogr.* **1969**, *128*, 352.
[37] W. M. Meier, D. H. Olson, C. Bärlocher, *Atlas of Zeolite Structure Types*, Elsevier, London, **1996**.
[38] G. V. Tsitsishvili, *Adv. Chem. Ser.* **1973**, *121*, 291.
[39] D. W. Breck, E. M. Flanigen, *Molecular Sieves*, Society of Chemical Industry, London, **1968**, p. 47.
[40] H. Hoyer, W. Peperle, *Z. Elektrochem.* **1958**, *62*, 61.
[41] L. Silverman, K. Trego, W. Houk, M. E. Shideler, *J. Appl. Chem.* **1958**, *8*, 616.
[42] M. Akiyama, T. Watanabe, M. Kakihana, *J. Phys. Chem.* **1986**, *90*, 1752.
[43] Non integral numbers are possible in principle but do not paly a role in this study.
[44] F. Binder, G. Calzaferri, N. Gfeller, *Sol. Energy Mater. Sol. Cells* **1995**, *38*, 175.
[45] C. L. Angell, *J. Phys. Chem.* **1973**, *77*, 222.
[46] P. K. Dutta, D. C. Shieh, M. Puri, *Zeolites* **1988**, *8*, 306.
[47] R. G. Buckley, H. W. Deckman, J. M. Newsam, J. A. McHenry, P. D. Persans, H. Witzke, *Mat. Res. Soc. Symp. Proc.* **1988**, *111*, 141.
[48] H. W. Deckman, J. A. Creighton, R. G. Buckley, J. M. Newsam, *Mater. Res. Soc. Symp. Proc.* **1991**, *233*, 295.
[49] W. Pilz, *Z. Phys. Chem.* **1990**, *271*, 219.
[50] A. J. M. de Man, R. A. van Santen, *Zeolites* **1992**, *12*, 269.
[51] J. E. Katon, E. R. Lippincott, *Spectrochim. Acta* **1959**, 627.
[52] The fluorescence intensity of DPH increases by a factor of 5, when cooling a DPH-zeolite L sample from rt to 77 K. From this follows that the rt fluorescence quantum yield cannot exceed 0.2.

[53] R. M. Barrer, J. A. Lee, *Surf. Sci.* **1968**, *12*, 341.
[54] T. Förster, *Fluoreszenz Organischer Verbindungen*, Vandenhoeck & Ruprecht, Göttingen, **1951**.
[55] S. K. Chattopadhyay, P. K. Das, G. L. Hug, *J. Am. Chem. Soc.* **1982**, *104*, 4508.
[56] M. Rinke, H. Guesten, *Ber. Bunsen-Ges. Phys. Chem.* **1986**, *90*, 439.
[57] W. Müller, *Liebigs Ann. Chem.* **1974**, 334.
[58] U. Fiedeldei, Ph.D. Thesis, Freie University of Berlin, Germany, **1988**.
[59] a) E. Vogelmann, Ph.D. Thesis, University of Stuttgart, Germany, **1974**; b) K. H. Drexhage, *J. Res. NBS A* **1976**, *80A*, 421; c) P. Iwa, U. E. Steiner, E. Vogelmann, H. E. A. Kramer, *J. Phys. Chem.* **1982**, *86*, 1277.
[60] N. Gfeller, Ph.D Thesis, University of Bern, Switzerland, **1992**.

Received: March 23, 2000 [F2303]

  0947-6539/00/0618-3470 $ 17.50+.50/0